(Fluoroalkyl)phosphine Complexes of Rhodium and Iridium. Synthesis and Reactivity Properties of $[(dfepe)Ir(\mu\text{-}Cl)]_2$

R. Chris Schnabel and Dean M. Roddick*

Chemistry Department, Box 3838, University of Wyoming, Laramie, Wyoming 82071

Received October 9, 1992

The synthesis, structure, and reactivity properties of iridium and rhodium (fluoroalkyl)phosphine dimeric complexes $[(dfepe)M(\mu\text{-}Cl)]_2$ (dfepe = $(C_2F_5)_2PCH_2CH_2P(C_2F_5)_2$; M = Rh (**1**); M = Ir (**2**)) are described. Complexes **1** and **2** are prepared in high yield from the displacement of cyclooctadiene from $[(cod)M(\mu\text{-}Cl)]_2$. X-ray diffraction studies reveal that **1** and **2** are isomorphous with identical $M_2(\mu\text{-}Cl)_2$ dihedral hinge angles of 128°. Complexes **1** and **2** exhibit high thermal stability and do not undergo oxidative addition reactions with H_2, O_2, or alkyl halides. Although chloride abstraction or alkylation of **2** was unsuccessful, CpIr(dfepe) was prepared in good yield from the reaction of **2** with TlCp in refluxing THF. Addition of both donor and acceptor ligands to **2** produces monomeric products. Treatment of **2** with excess diethylamine affords $(dfepe)Ir(NEt_2H)Cl$ (**4**), a surprisingly stable alkylamine complex which has been structurally characterized. Carbonylation reactions of both **1** and **2** are concentration- and solvent-dependent. In dilute acetone solutions, $(dfepe)M(CO)Cl$ products are observed (M = Ir (**5**), $\nu(CO)$ = 2076 cm^{-1}; M = Rh (**6**), $\nu(CO)$ = 2093 cm^{-1}), which could not be isolated due to reversible CO loss in the absence of a CO atmosphere. At higher solution concentrations dfepe loss is observed concomitant with the formation of new solution species tentatively formulated as solvated oligomers, $[(CO)_2M(\mu\text{-}Cl)(solv)]_x$. Crystal data for **1** (−100 °C): trigonal, $P3_221$, with a = 14.215(2) Å, c = 34.545(8) Å, V = 6045(2) Å^3, Z = 6, R = 6.32%, and R_w = 6.64%. Crystal data for **2** (−100 °C): trigonal, $P3_221$, with a = 14.159(2) Å, c = 34.649(7) Å, V = 6016(2) Å^3, Z = 6, R = 6.28%, and R_w = 6.49%. Crystal data for **4** (−100 °C): orthorhombic, $P2_12_12_1$, with a = 11.262(2) Å, b = 14.093(2) Å, c = 15.274(2) Å, V = 2424.2(6) Å^3, Z = 4, R = 3.76%, and R_w = 4.12%.

Introduction

The coordination chemistry of rhodium and iridium phosphine complexes plays a major role in our understanding of basic organometallic reactions and homogeneous catalytic processes.[1] Complexes of the general form $(R_3P)_2M(L)X$ (L = CO or R_3P, X = halide or hydride) have received considerable attention as efficient hydrogenation,[2] hydroformylation,[3] and decarbonylation catalysts.[4] In contrast to the wide range of reactivity found for electron-rich group IX phosphine complexes, the corresponding chemistry of electron-poor rhodium and iridium carbonyl systems is relatively limited.

We have reported the synthesis and coordination properties of the (fluoroalkyl)phosphine chelate $(C_2F_5)_2PCH_2CH_2P(C_2F_5)_2$ ("dfepe").[5] Spectroscopic, structural, and reactivity data have indicated that this ligand possesses an unusual combination of steric and electronic properties and may serve as a sterically-demanding, electronic analogue to conventional carbonyl systems.[6] In view of the extensive chemistry of electron-rich rhodium and iridium systems, we have begun a systematic study of the (fluoroalkyl)phosphine chemistry of group IX metals with the goal of designing novel electrophilic counterparts to established donor phosphine systems. Herein we report our initial studies on the synthesis and coordination properties of iridium and rhodium (fluoroalkyl)phosphine complexes.

Results and Discussion

Synthesis and Structure of $[(dfepe)M(\mu\text{-}Cl)]_2$ (M = Rh, Ir). The stoichiometry and molecularity of rhodium and iridium phosphine halide systems $[(R_3P)_nMCl]_x$ reflect a combination of ligand steric and electronic properties, with sterically-demanding poor donor ligands favoring dimeric $[(R_3P)_2M(\mu\text{-}Cl)]_2$ structures.[7] For example, while both PCy_3 (θ = 170°)[8] and PF_3 (θ = 104°) readily form the monomeric phosphine complexes $(Cy_3P)_2RhCl$[9] and $(F_3P)_4RhCl$,[10] $[((C_6F_5)_3P)_2Rh(\mu\text{-}Cl)]_2$ is the sole product obtained in the reaction of $[(C_2H_4)_2Rh(\mu\text{-}Cl)]_2$ with excess $P(C_6F_5)_3$ (θ = 184°).[11] In accordance with these trends, the reactions of $[(cod)M(\mu\text{-}Cl)]_2$ complexes with excess dfepe (θ = 129°)[6a] exclusively afford the dimers $[(dfepe)M(\mu\text{-}Cl)]_2$ (M = Rh, **1**; Ir, **2**) in nearly quantitative yield (eq 1). Both **1** and **2**

$$[(cod)M(\mu\text{-}Cl)]_2 + 2dfepe \xrightarrow[CH_2Cl_2,\ room\ temp]{-2cod} [(dfepe)M(\mu\text{-}Cl)]_2 \quad (1)$$
$$M = Rh\ (\mathbf{1})$$
$$M = Ir\ (\mathbf{2})$$

exhibit remarkable thermal stability compared to known phosphine analogues; no detectable decomposition or solvent C–H addition products of **2** are found after several days at 150 °C in cyclohexane. The high thermal stability of the Ir(I) complex **2** is particularly significant in light of facile C–H ligand metallation reactions found for Ir(I) aryl- and alkyl-substituted phosphine

(1) (a) Jardine, F. H. In *Chemistry of the Platinum Group Metals*; Hartley, F. R., Ed.; Elsevier: New York, 1991; Chapter 13. (b) Dickson, R. S. *Homogeneous Catalysis with Compounds of Rhodium and Iridium*; D. Reidel Publishing Co.: Dordrecht, Holland, 1985.
(2) (a) Collman, J. P.; Hegedus, L. S.; Norton, J. R.; Finke, R. G. *Principles and Applications of Organotransition Metal Chemistry*, 2nd ed.; University Science Books: Mill Valley, CA, 1987; Chapter 10 and references therein.
(3) Pruett, R. L. *Adv. Organomet. Chem.* **1979**, *17*, 1.
(4) (a) Abu-Hasanayn, F.; Goldman, M. E.; Goldman, A. S. *J. Am. Chem. Soc.* **1992**, *114*, 2520. (b) Doughty, D. H.; Pignolet, L. H. In *Homogeneous Catalysis with Metal Phosphine Complexes*; Pignolet, L. H., Ed.; Plenum: New York, 1983; Chapter 11.
(5) Ernst, M. F.; Roddick, D. M. *Inorg. Chem.* **1989**, *28*, 1624.
(6) (a) Ernst, M. F.; Roddick, D. M. *Organometallics* **1990**, *9*, 1586. (b) Koola, J. D.; Roddick, D. M. *J. Am. Chem. Soc.* **1991**, *113*, 1450.
(7) (a) Jardine, F. H.; Sheridan, P. S. *Comprehensive Coordination Chemistry*; Wilkinson, G., Stone, F. G. A., Abel, E. W., Eds.; Pergamon: Oxford, England, 1982; Vol. 4, pp 906–928 and references cited therein.
(8) Tolman, C. A. *Chem. Rev.* **1977**, *77*, 313.
(9) Van Gaal, H. L. M.; Van den Bekerom, F. L. A. *J. Organomet. Chem.* **1977**, *134*, 237.
(10) Bennett, M. A.; Turney, T. W. *Aust. J. Chem.* **1973**, *26*, 2321.
(11) Kemmitt, R. D. W.; Nichols, D. I.; Peacock, R. D. *J. Chem. Soc. A* **1968**, 1898.

0020-1669/93/1332-1513$04.00/0

Table I. Summary of $[L_2M(\mu\text{-}Cl)]_2$ Structural Parameters

complex	λ,[a] deg	M–M, Å	av M–Cl, Å	av L–M–L, deg	Cl–M–Cl, deg	ref
$[(Ph_3P)_2Rh(\mu\text{-}Cl)]_2$	180	3.662(2)	2.409(2)	96.3(1)	81.1(1)	16
$[(cod)Rh(\mu\text{-}Cl)]_2$	180	3.50	2.38	90	85	15e
$[(dfepe)Rh(\mu\text{-}Cl)]_2$	128	3.219(4)	2.398(4)	84.9(2)	83.5(1)	this work
$[(dfepe)Ir(\mu\text{-}Cl)]_2$	128	3.236(4)	2.376(10)	84.8(4)	81.4(4)	this work
$[(CO)_2Rh(\mu\text{-}Cl)]_2$	124	3.12	2.35	91	85	15f
$[(C_2H_4)_2Rh(\mu\text{-}Cl)]_2$	116	3.02	2.40		84	17
$[(F_3P)_2Ir(\mu\text{-}Cl)]_2$	107	2.941(1)	2.413(5)			18
$[(cod)Ir(\mu\text{-}Cl)]_2$[20]	106	2.910(1)	2.401(4)	88.3	84.2(2)	19

[a] λ is defined as the $M_2(\mu\text{-}Cl)_2$ core dihedral angle.

Table II. Summary of Crystallographic Data for $[(dfepe)M(\mu\text{-}Cl)]_2$ and $(dfepe)Ir(NEt_2H)Cl$

	$C_{20}H_8Cl_2F_{40}P_4Rh_2$	$C_{20}H_8Cl_2F_{40}P_4Ir_2$	$C_{14}H_{15}ClF_{20}IrNP_2$
space group	$P3_221$ (No. 154)	$P3_221$ (No. 154)	$P2_12_12_1$ (No. 19)
temp, °C	−100	−100	−100
a, Å	14.215(2)	14.159(2)	11.262(2)
b, Å			14.093(2)
c, Å	34.545(8)	34.649(7)	15.274(2)
V, Å^3	6045(2)	6016(2)	2424.2(6)
Z	6	6	4
ρ_{calc}, g/cm^3	2.322	2.629	2.372
fw	1408.9	1587.4	1731.7
λ, Å	0.710 73	0.710 73	0.710 73
μ, mm^{-1}	1.30	7.10	5.88
T_{max}/T_{min}	1.16	2.24	2.65
R,[a] %	6.32	6.28	3.76
R_w,[b] %	6.64	6.49	4.12

[a] $R = \sum||F_o| - |F_c||/\sum|F_o|$. [b] $R_w = \sum|w^{1/2}(F_o - F_c)|/\sum[(F_o)w^{1/2}]$.

complexes such as $(Ph_3P)_3IrCl$[12] and $(^tBu_3P)_2IrCl$.[13] In contrast to the well-documented oxidative addition chemistry of electron-rich M(I) systems, complexes **1** and **2** are air-stable and do not react with H_2, O_2, MeI, $BrCH_2CH_2Br$, or allyl chloride. Dinuclear oxidative addition[14] of CH_2Cl_2 or CH_2I_2 is also not observed.

The conformation of the $M_2(\mu\text{-}Cl)_2$ core in **1** and **2** is of some interest. Although crystallographic studies of a number of chloro-bridged dimers with both planar and hinged $M_2(\mu\text{-}Cl)_2$ cores have been reported,[15-19] no obvious correlation between core geometry and the nature of the ancillary ligands is apparent (see Table I).[21] The only direct comparison of metal-based factors is provided by structural studies of $[(cod)M(\mu\text{-}Cl)]_2$ (M = Rh, Ir) complexes. Whereas $Rh_2(\mu\text{-}Cl)_2$ is strictly planar (Rh–Rh = 3.662 Å),[15e] the iridium analogue exhibits a highly bent $Ir_2(\mu\text{-}Cl)_2$ geometry with a hinge angle λ of 106° and a Ir–Ir distance of 2.910 Å.[19,20] The solid state structures of both **1** and **2** have been determined in order to test the generality of this vertical periodic trend. **1** and **2** are isomorphous, crystallizing in the trigonal space group $P3_221$. Data collection parameters are summarized in Table II. Atomic coordinates and selected metrical parameters are given in Tables III–V. In contrast to the $[(cod)M(\mu\text{-}Cl)]_2$ systems, **1** and **2** are isostructural. A representative ORTEP view of the rhodium derivative is given in Figure 1. The average Rh–P (2.152(5) Å) and Ir–P (2.15(1) Å) bond lengths found for **1** and **2** are significantly shorter (0.15–0.20 Å) than typical donor phosphine M–P bond lengths in 4-coordinate rhodium and iridium structures,[22] and are comparable to the average M–P value reported for the iridium trifluorophosphine

Table III. Selected Atomic Coordinates (×10^4) and Equivalent Isotropic Displacement Coefficients (Å^2 × 10^3) for $[(dfepe)Rh(\mu\text{-}Cl)]_2$ (**1**)

atom	*x*	*y*	*z*	*U*(eq)[a]
Rh(1)	9818(1)	3209(1)	634(1)	23(1)
Rh(2)	9215(1)	4577(1)	1225(1)	24(1)
Cl(1)	10574(3)	5121(3)	728(1)	30(2)
Cl(2)	9604(3)	3141(3)	1324(1)	28(2)
P(1)	10000(3)	3332(3)	13(1)	30(2)
P(2)	9136(4)	1488(3)	544(1)	33(2)
P(3)	8865(4)	5867(4)	1142(1)	30(2)
P(4)	8013(4)	4061(4)	1676(1)	29(2)
C(1)	9709(15)	2062(14)	−299(5)	38(9)
C(2)	8906(16)	1090(14)	33(4)	44(9)
C(3)	11372(15)	4313(16)	−226(5)	40(5)
C(5)	9131(15)	3794(15)	−257(5)	37(5)
C(7)	10008(20)	882(20)	664(7)	66(7)
C(9)	7708(18)	569(18)	764(6)	56(6)
C(11)	8018(16)	5936(14)	1520(6)	45(10)
C(12)	7315(17)	4844(16)	1724(5)	48(12)
C(13)	8098(16)	5754(16)	684(5)	44(5)
C(15)	9985(16)	7308(17)	1099(6)	45(5)
C(17)	8479(16)	3974(15)	2185(5)	37(5)
C(19)	6804(14)	2611(15)	1669(5)	35(5)

[a] Equivalent isotropic *U* defined as one-third of the trace of the orthogonalized U_{ij} tensor.

Table IV. Atomic Coordinates (×10^4) and Equivalent Isotropic Displacement Coefficients (Å^2 × 10^3) for $[(dfepe)Ir(\mu\text{-}Cl)]_2$ (**2**)

atom	*x*	*y*	*z*	*U*(eq)[a]
Ir(1)	6615(1)	9821(1)	8960(1)	28(1)
Ir(2)	4627(1)	9210(1)	9554(1)	29(1)
Cl(1)	5470(7)	10577(8)	9065(2)	38(4)
Cl(2)	6448(7)	9624(7)	9641(2)	34(4)
P(1)	6671(7)	10008(8)	8340(2)	34(4)
P(2)	7656(9)	9144(9)	8866(3)	41(5)
P(3)	2974(8)	8849(8)	9471(3)	36(4)
P(4)	3943(8)	7998(8)	10005(2)	29(4)
C(1)	7618(33)	9632(34)	8099(10)	47(10)
C(2)	7819(30)	8925(31)	8356(9)	41(9)
C(3)	6993(31)	11320(31)	8098(10)	39(9)
C(5)	5316(36)	9138(38)	8060(12)	60(12)
C(7)	9175(39)	10111(41)	8992(14)	64(13)
C(9)	7158(34)	7730(35)	9102(11)	49(11)
C(11)	2096(33)	8075(30)	9858(9)	44(9)
C(12)	2487(29)	7363(30)	10041(10)	36(8)
C(13)	2320(34)	8081(37)	8994(11)	55(11)
C(15)	2728(40)	9993(39)	9432(13)	62(13)
C(17)	4515(30)	8462(31)	10499(10)	39(9)
C(19)	4214(30)	6832(29)	10002(10)	36(9)

[a] Equivalent isotropic *U* defined as one-third of the trace of the orthogonalized U_{ij} tensor.

(12) Bennett, M. A.; Milner, D. L. *J. Am. Chem. Soc.* **1969**, *91*, 6983.
(13) Dahlenburg, L.; Yardimcioglu, A. *J. Organomet. Chem.* **1986**, *299*, 149.
(14) Ball, G. E.; Cullen, W. R.; Fryzuk, M. D.; James, B. R.; Rettig, S. J. *Organometallics* **1991**, *10*, 3767.
(15) (a) Bonnet, J. J.; Jeannin, Y.; Kalck, P.; Maisonnat, A.; Poilblanc, R. *J. Inorg. Chem.* **1975**, *14*, 743. (b) Drew, M. G. B.; Nelson, S. M.; Sloan, M. *J. Chem. Soc., Dalton Trans.* **1973**, 1484. (c) Coetzer, J.; Gafner, G. *Acta Crystallogr., Sect. B* **1970**, *26*, 985. (d) Bateman, L. R.; Maitlis, P. M.; Dahl, L. F. *J. Am. Chem. Soc.* **1969**, *91*, 7292. (e) Ibers, J. A.; Snyder, R. G. *Acta Crystallogr.* **1962**, *15*, 923. (f) Dahl, L. F.; Martell, C.; Wampler, D. L. *J. Am. Chem. Soc.* **1961**, *83*, 1761.
(16) Curtis, M. D.; Butler, W. M.; Greene, J. *Inorg. Chem.* **1978**, *17*, 2928.
(17) Klanderman, K.; Dahl, L. F. Quoted in ref 15d.
(18) Hitchcock, P. B.; Morton, S.; Nixon, J. F. *J. Chem. Soc., Dalton Trans.* **1985**, 1295.
(19) Cotton, F. A.; Lahuerta, P.; Sanau, M.; Schwotzer, W. *Inorg. Chim. Acta* **1986**, *120*, 153.
(20) The dihedral angle of 86° cited for $[(cod)Ir(\mu\text{-}Cl)]_2$ in ref 19 is incorrect. Reevaluation of least-squares molecular planes for each metal center including all ligated atoms yields a value of λ = 106°. The dihedral angle between planes defined by just the Ir and Cl atoms is 109°.
(21) (a) Norman, J. G.; Gmur, D. J. *J. Am. Chem. Soc.* **1977**, *99*, 1446. (b) Summerville, R. H.; Hoffmann, R. *J. Am. Chem. Soc.* **1976**, *98*, 7240.
(22) Orpen, A. G.; Brammer, L.; Allen, F. H.; Kennard, O.; Watson, D. G.; Taylor, R. *J. Chem. Soc., Dalton Trans.* **1989**, S1.

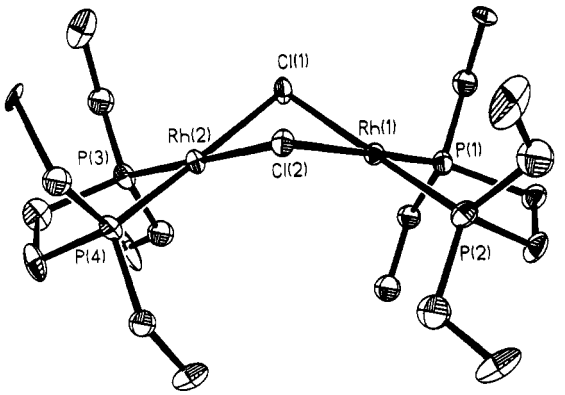

Figure 1. Molecular structure of $[(dfepe)Rh(\mu\text{-}Cl)]_2$ (**1**) with the atom-labeling scheme. Fluorine atoms are omitted for clarity; thermal ellipsoids are shown at the 30% probability level.

Table V. Selected Distances (Å) and Angles (deg) for $[(dfepe)Rh(\mu\text{-}Cl)]_2$ (**1**) and $[(dfepe)Ir(\mu\text{-}Cl)]_2$ (**2**)

	M = Rh	M = Ir
	Bond Distances	
M(1)–Cl(1)	2.394(5)	2.375(13)
M(1)–Cl(2)	2.399(4)	2.374(7)
M(2)–Cl(1)	2.405(4)	2.393(9)
M(2)–Cl(2)	2.392(6)	2.360(10)
M(1)–P(1)	2.157(4)	2.159(7)
M(1)–P(2)	2.156(5)	2.148(15)
M(2)–P(3)	2.144(7)	2.150(12)
M(2)–P(4)	2.151(5)	2.158(9)
	Bond Angles	
Cl(1)–M(1)–Cl(2)	83.5(1)	81.4(4)
Cl(1)–M(2)–Cl(2)	83.4(2)	81.3(3)
P(1)–M(1)–P(2)	85.2(2)	85.0(4)
P(1)–M(1)–Cl(1)	94.3(2)	95.1(4)
P(1)–M(1)–Cl(2)	177.4(2)	176.2(4)
P(2)–M(1)–Cl(1)	179.5(2)	179.7(3)
P(2)–M(1)–Cl(2)	97.0(2)	98.5(4)
P(3)–M(2)–P(4)	84.5(2)	84.5(4)
P(3)–M(2)–Cl(1)	97.0(2)	98.1(4)
P(3)–M(2)–Cl(2)	179.5(2)	179.4(3)
P(4)–M(2)–Cl(1)	178.4(2)	177.3(4)
P(4)–M(2)–Cl(2)	95.1(2)	96.1(4)
M(1)–Cl(1)–M(2)	84.2(1)	85.5(4)
M(1)–Cl(2)–M(2)	84.4(1)	84.5(4)

complex, $[(F_3P)_2Ir(\mu\text{-}Cl)]_2$ (2.134(5) Å).[18] This substantial shortening of M–P bond lengths relative to donor phosphine systems is typical for the dfepe ligand and has been previously ascribed to a combination of multiple bonding and phosphorus hybridization effects.[6a] M–Cl bond distances for **1** and **2** fall within the range reported for other $[L_2M(\mu\text{-}Cl)]_2$ complexes and appear to be largely insensitive to the nature of the trans ligands, as noted previously.[16] Other than the two planar structural examples listed in Table I, **1** and **2** exhibit the largest λ values yet reported. It is likely that for these systems fluoroalkylphosphine steric interactions dominate any relative bonding advantage iridium may have over rhodium in a highly-bent $M_2(\mu\text{-}Cl)_2$ geometry.[21]

Synthesis of CpIr(dfepe) and (dfepe)Ir(NEt$_2$H)Cl. Although the M-Cl bond lengths for **1** and **2** are quite normal, reactivity studies indicate a reduced chloride lability for these electron-poor compounds relative to electron-rich M(I) halide systems. No reaction between **2** and halide abstraction reagents such as $AgBF_4$, TlCl, or Me_3SiOTf in the presence of coordinating solvents and/or excess dfepe to give $[(dfepe)Ir(solv)_2]^+$ or $[(dfepe)_2Ir]^+$ products paralleling the chemistry typical of donor phosphine analogues is observed. No characterizable products were obtained from the reaction of **2** with MeMgBr. However, metathesis of the chloride ligands of **2** with TlCp takes place in refluxing THF to give CpIr(dfepe) (**3**) as a stable orange solid in 60% yield (eq 2).

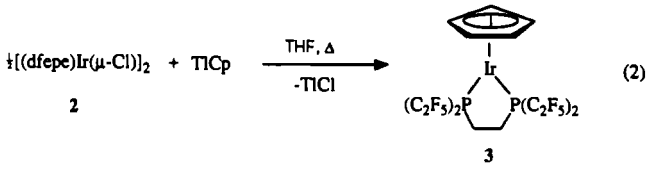

2 (2)

3

Donor ligand addition reactions to the iridium dimer **2** are facile. Although iridium(I) complexes generally exhibit a low affinity toward alkylamine ligands, the reaction of **2** with neat diethylamine cleanly affords (dfepe)Ir(NEt$_2$H)Cl (**4**) (eq 3).

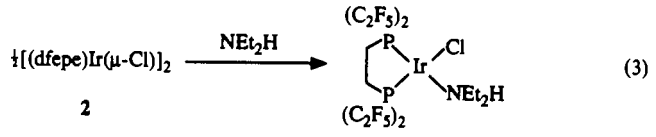

2 (3)

4

Treatment of **2** with excess triethylamine, however, does not yield a tertiary amine adduct. The formulation of **4** is consistent with spectroscopic data. The integrity of the secondary amine ligand is clearly indicated by the ^1H NMR spectrum, which exhibits a broad amine hydrogen resonance at δ 3.72. The CH_2 amine protons are diastereotopic and appear as highly-coupled multiplets at 2.54 and 3.03 ppm in benzene (see Experimental Section). These amine methylene units serve as a convenient probe for dynamic behavior: If amine dissociation were facile on the NMR time scale, one would expect collapse of these resonances to a simple quartet due to rapid pyramidal inversion of the free amine.[23] However, no broadening or coalescence is observed in toluene-d_8 at temperatures up to 150 °C, indicating that amine dissociation does not occur at a significant rate under these conditions. In benzene solution no H–D exchange occurs at 20 °C between the amine proton of **4** and excess D_2O over a period of several days. In acetone, however, H–D exchange with excess D_2O is complete within 30 min.[24] The amine-substituted iridium(I) center of **4** is expected to be more electron-rich than the parent chloride dimer **2**. Nevertheless, oxidative addition of H_2 to this 16-electron complex is also not observed.

Crystal Structure of (dfepe)Ir(NEt$_2$H)Cl. The solid state structure of **4** has been determined in order to provide an internal comparison of Ir–P and Ir–N bonding. (dfepe)Ir(NEt$_2$H)Cl is also notable for being the first structurally-characterized example of an iridium alkylamine complex where the amine is not part of a chelating ligand system. A summary of metrical data is given in Table VII. As expected, the ligand environment about the iridium is square-planar, with an L–M–L angular sum of 360.4° (Figure 2). The mean deviation from the least-squares plane defined by the five atoms in the coordination core is 0.0814 Å. The Ir(1)–N(1) bond distance of 2.185(8) Å is comparable to that reported for 4-coordinate Ir(I) alkylamine complexes $[o\text{-}C_6H_4(PPh_2)(NMe_2)]Ir(CO)Cl$ (2.180(5) Å)[25] and $[o,p\text{-}C_6H_3(CH_2NMe_2)_2]Ir(cod)$ (2.164(3) Å).[26] Ir(I)–N(R)$_3$ bond distances in 5- and 6-coordinate complexes are considerably longer (*ca.* 0.2 Å),[27] perhaps reflecting the relatively poor coordination

(23) Bushweller, C. H. In *Acyclic Organonitrogen Stereodynamics*; Lambert, J. B.; Takeuchi, Y., Eds.; VCH Publishers, Inc., New York, 1992; Chapter 1.

(24) The amine methylene units of **4** remain diastereotopic in acetone in the presence of excess H_2O, indicating that rapid amine exchange does not occur under the conditions of H–D exchange.

(25) Roundhill, D. M.; Bechtold, R. A.; Roundhill, S. G. N. *Inorg. Chem.* **1980**, *19*, 284.

(26) van der Zeijden, A. A. H.; van Koten, G.; Luijk, R.; Nordemann, R. A.; Spek, A. L. *Organometallics* **1988**, *7*, 1549.

(27) (a) Bianchini, C.; Farnetti, E.; Graziani, M.; Nardin, G.; Vacca, A.; Zanobini, F. *J. Am. Chem. Soc.* **1990**, *112*, 9190. (b) van der Zeijden, A. A. H.; van Koten, G.; Wouters, J. M. A.; Wijsmuller, W. F. A.; Grove, D. M.; Smeets, W. J. J.; Spek, A. L. *J. Am. Chem. Soc.* **1988**, *110*, 5354.

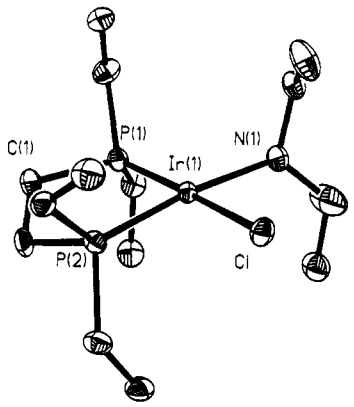

Figure 2. Molecular structure of (dfepe)Ir(NEt_2H)Cl (**4**) with the atom-labeling scheme. Fluorine atoms are omitted for clarity; thermal ellipsoids are shown at the 30% probability level.

Table VI. Atomic Coordinates ($\times 10^4$) and Equivalent Isotropic Displacement Coefficients ($Å^2 \times 10^3$) for (dfepe)Ir(NEt_2H)Cl (**4**)

atom	*x*	*y*	*z*	*U*(eq)[a]
Ir(1)	9655(1)	520(1)	9081(1)	26(1)
P(1)	9042(2)	-858(1)	9485(1)	32(1)
P(2)	10892(2)	-276(1)	8282(1)	30(1)
Cl	10503(2)	1968(1)	8631(1)	39(1)
N(1)	8299(8)	1371(6)	9736(5)	48(2)
C(1)	9885(7)	-1857(5)	9011(6)	40(2)
C(2)	10513(9)	-1540(5)	8197(6)	42(2)
C(3)	7421(9)	-1208(7)	9286(7)	47(3)
C(5)	9023(9)	-1246(7)	10687(6)	48(3)
C(7)	11090(8)	45(7)	7081(5)	41(2)
C(9)	12527(7)	-396(6)	8602(5)	37(2)
C(11)	7657(17)	2024(16)	9289(10)	136(9)
C(12)	7252(10)	1863(9)	8396(7)	58(3)
C(21)	8459(8)	1533(7)	10704(6)	45(3)
C(22)	9594(10)	1997(8)	10878(9)	70(4)

[a] Equivalent isotropic *U* defined as one-third of the trace of the orthogonalized U_{ij} tensor.

Table VII. Selected Distances (Å) and Angles (deg) for (dfepe)Ir(NEt_2H)Cl (**4**)

	Bond Distances		
Ir(1)-P(1)	2.151(2)	Ir(1)-P(2)	2.165(2)
Ir(1)-Cl	2.356(2)	Ir(1)-N(1)	2.185(8)
	Bond Angles		
P(1)-Ir(1)-P(2)	84.3(1)	P(1)-Ir(1)-Cl	174.7(1)
P(1)-Ir(1)-N(1)	98.0(2)	P(2)-Ir(1)-Cl	91.4(1)
P(2)-Ir(1)-N(1)	172.9(2)	Ir(1)-P(1)-C(1)	114.3(3)
Ir(1)-P(1)-C(3)	119.5(3)	Ir(1)-P(1)-C(5)	122.4(3)
C(1)-P(1)-C(3)	103.4(4)	C(1)-P(1)-C(5)	99.4(4)
C(3)-P(1)-C(5)	93.9(4)	Ir(1)-P(2)-C(2)	113.1(3)
Ir(1)-P(2)-C(7)	119.7(3)	Ir(1)-P(2)-C(9)	121.4(3)
C(2)-P(2)-C(7)	101.0(4)	C(2)-P(2)-C(9)	99.0(4)
C(7)-P(2)-C(9)	98.9(4)	Ir(1)-N(1)-C(11)	121.0(8)
Ir(1)-N(1)-C(21)	116.7(6)	C(11)-N(1)-C(21)	117.1(10)

properties of tertiary amine ligands in more sterically-congested environments. Although the amine hydrogen was not located, the conformation of the Et_2N fragment indicates that it is oriented approximately toward P(1) (Figure 3). Within experimental uncertainty the Ir(1)-P(2) bond distance is essentially equivalent to that of Ir(1)-N(1). After correcting for librational effects (riding model), the adjusted bond distances are 2.168 and 2.202 Å for Ir(1)-P(2) and Ir(1)-N(1), respectively. The similarity between M-P and M-N bond lengths is counter to expectations based on a simple covalent radii ordering ($r(P) - r(N) \approx 0.4$ Å),[28] but is in accord with the unusually short M-P bond distances found for **1** and **2**. A considerable difference between the hybridization of the nitrogen and phosphorus lone pairs is indicated

(28) Jolly, W. L. *Modern Inorganic Chemistry*, 2nd ed.; McGraw-Hill, Inc.: New York, 1991; p 54.

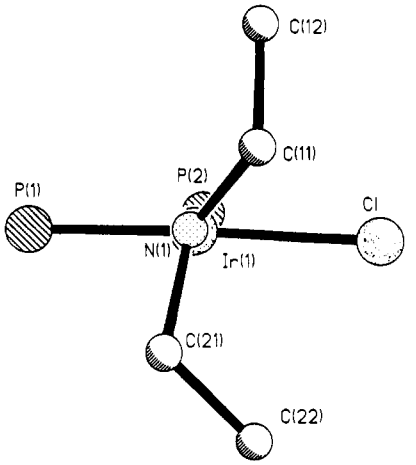

Figure 3. Projection of compound **4** along the N(1)-Ir(1) bond, showing the conformation of the NEt_2H ligand.

by the inter-substituent angles about the ligating heteroatoms. For nitrogen, the angle between the ethyl groups is 117°, considerably larger than the angles between the perfluoroethyl groups for dfepe (93.9 and 98.9°). The smaller angles found for the electronegative dfepe substituents follows Bent's rule[29] and indicate that there is considerably more "s" character in the lone pair orbitals of dfepe. Interestingly, the angular sum about nitrogen is 354.8° and is indicative of a nearly trigonal planar amine geometry.[30]

Carbonylation Reactions of [(dfepe)M(μ-Cl)]$_2$. The reaction of **2** with CO is both solvent- and concentration-dependent. In benzene solution, a single carbonyl band at 2083 cm^{-1} under 1 atm CO is observed which is assignable to (dfepe)Ir(CO)Cl (**5**) (eq 4). ^{13}C NMR data for the ^{13}CO labeled complex (dfepe)-

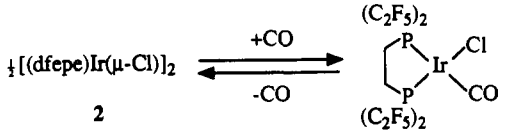

(4)

2 **5**

Ir(^{13}CO)Cl (δ 178.55, dd, $^2J_{PC}$ = 142, 8 Hz) confirm this formulation. Complex **5** slowly decarbonylates to re-form **2** under ambient conditions in the absence of a CO atmosphere and could not be isolated in a pure form. The high lability of CO found for (dfepe)Ir(CO)Cl is not surprising in view of the high value of ν(CO) for **5** relative to donor phosphine analogues such as (dppe)Ir(CO)Cl (ν(CO) = 1983 cm^{-1}).[31]

Carbonylation behavior of **2** in the more polar and potentially coordinating solvent acetone is more complex. Under dilute conditions ($[\mathbf{2}]_0$ = 1.02 mM, 590 Torr CO, 20 °C), a single carbonyl band at 2076 cm^{-1} due to **5** was observed (Figure 4). At a higher initial concentration of 5.02 mM under the same CO pressure, the solution became light green and two additional ν(CO) bands of nearly equal intensity at 2048 and 1965 cm^{-1} were observed. At $[\mathbf{2}]_0$ = 10.0 mM, a deep blue-green solution was obtained and the only ν(CO) bands present were those at 2048 and 1965 cm^{-1}. In a control experiment, treatment of [(cod)Ir(μ-Cl)]$_2$ in acetone with CO yielded a blue solution with identical ν(CO) bands, suggesting that a loss of dfepe had occurred; the ^{31}P NMR of **2** under CO confirmed the presence of free dfepe. The blue color observed in the carbonylations of both **2** and [(cod)Ir(μ-Cl)]$_2$ faded after 30 min to light orange without any

(29) Bent, H. A. *Chem. Rev.* **1961**, *61*, 275.
(30) Nearly trigonal planar secondary amine coordination has been reported previously for NEt_2H: Englehardt, L. M.; Gotsis, S.; Healy, P. C.; Kildea, J. D.; Skelton, B. W.; White, A. H. *Aust. J. Chem.* **1989**, *42*, 149.
(31) Johnson, C. E.; Eisenberg, R. *J. Am. Chem. Soc.* **1985**, *107*, 3148.
(32) Morris, D. E.; Tinker, H. B. *J. Organomet. Chem.* **1973**, *49*, C53.

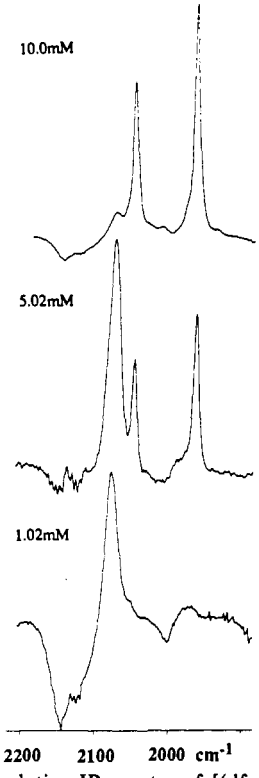

Figure 4. Difference solution IR spectra of $[(dfepe)Ir(\mu\text{-}Cl)]_2$ (**2**) in acetone under 1 atm of CO, at three different initial concentrations of **2**, $[\mathbf{2}]_0$.

concomitant changes in the infrared spectrum, and is therefore apparently due to a transient minor solution component.

The behavior of the rhodium dimer **1** in acetone under CO is similar. Under 1 atm CO, a band at 2093 cm^{-1} assigned to (dfepe)Rh(CO)Cl (**6**) is observed, together with two bands at 2061 and 1983 cm^{-1}. These latter two bands are shifted ca. 50 cm^{-1} to lower energy from values reported for $[(CO)_2Rh(\mu\text{-}Cl)]_2$.[31] In keeping with the generally lower affinity of rhodium toward CO relative to iridium, removal of CO from solutions of **1** results in complete decarbonylation to quantitatively regenerate **1** within 15 min at 20 °C.

The identity of the carbonylation products of **1** and **2** and $[(cod)Ir(\mu\text{-}Cl)]_2$ in acetone is uncertain. Although $[(CO)_2Rh(\mu\text{-}Cl)]_2$ is well-known, the corresponding iridium derivative has not been characterized. $(CO)_3IrCl$ has been reported as the product of $[(cod)Ir(\mu\text{-}Cl)]_2$ with CO (ν(CO) = 2140, 2070 cm^{-1}); however, an alternate synthesis of crystallographically-characterized $(CO)_3IrCl$ with substantially different chemical and spectroscopic properties places this claim in doubt.[33] Thus far efforts to isolate and fully characterize this product have been unsuccessful. ^{13}C NMR studies using ^{13}CO were similarly inconclusive due to rapid exchange between the solution species and ambient CO down to −80 °C. Since a simple equilibrium between **5** and monomeric $(CO)_3IrCl$ or $(CO)_2$(acetone)IrCl under a constant pressure of CO is also not consistent with the observed metal concentration dependence, we suggest the carbonylation products of **1**, **2** and $[(cod)Ir(\mu\text{-}Cl)]_2$ in acetone are most likely solvated oligomers, $[(CO)_2M(\mu\text{-}Cl)(solv)]_x$.

Summary. (Fluoroalkyl)phosphine complexes of rhodium and iridium exhibit reactivity patterns which are distinct from donor phosphine analogues in a number of respects. The electron-poor nature of the M(I) centers of **1** and **2** clearly prevents simple oxidative addition reactions. However, it is not obvious whether the considerable thermal stability of the iridium complex **2** is due to the avoidance of this decomposition pathway, the intrinsic inertness of phosphine substituent C–F bonds, or a combination of these two factors.

The formation of a stable iridium diethylamine complex **4** from **2** is unusual from the standpoint of typical Ir(I) ligand affinity trends, but may be understood from the standpoint of providing additional electron density to the electrophilic metal center. The substantially lowered affinity of **1** and **2** toward carbon monoxide is in accord with this simple view. We are currently examining the electrophilic properties of **1** and **2** in more detail as well as related, potentially more reactive, monomeric and dimeric (dfepe)M group IX systems.

Experimental Section

General Procedures. All manipulations were conducted under an atmosphere of nitrogen by using Schlenk, high vacuum line and/or glovebox techniques. Dry, oxygen-free solvents were vacuum distilled prior to use. Elemental analyses were performed by Desert Analytics. Infrared spectra were recorded on a Mattson Cygnus 100 or Perkin-Elmer 1600 FTIR instrument as Nujol mulls, unless otherwise noted. NMR spectra were obtained with a JEOL JMN-FX270 or GSX-400 instrument. ^{19}F spectra were referenced to CF_3CO_2Et as an internal standard (−75.32 ppm vs $CFCl_3$ with downfield chemical shifts taken to be positive). ^{31}P spectra were referenced to a 85% H_3PO_4 external standard. $[(cod)M(\mu\text{-}Cl)]_2$ (M = Rh, Ir) complexes were prepared following literature procedures.[34] $(C_2F_5)_2P\,CH_2CH_2P(C_2F_5)_2$ (dfepe) was prepared as described previously.[5]

$[(dfepe)Rh(\mu\text{-}Cl)]_2$ (1). To a room temperature solution of $[(C_8H_{12})Rh(\mu\text{-}Cl)]_2$ (0.502 g, 1.020 mmol) in 25 mL of toluene was added dfepe (1.327 g, 2.346 mmol) dropwise via syringe. The solution initially became dark red upon addition and then gradually lightened and began to precipitate an orange crystalline solid. After 2 h the precipitate was filtered off, washed twice with petroleum ether, and dried under vacuum for 30 min. The isolated yield of **1** was 1.346 g (92%). Anal. Calcd for $C_{20}H_8Cl_2F_{40}P_4Rh_2$: C, 17.06; H, 0.57. Found: C, 17.35; H, 0.49. IR (cm^{-1}): 1339 w, 1297 w, 1332 m, 1122 m, 966 m, 807 w, 750 w, 722 w, 711 w. ^1H NMR (acetone-d_6, 269.7 MHz, 20 °C): δ 2.68 (m, PCH_2). ^{31}P NMR (acetone-d_6, 161.9 MHz, 20 °C): δ 100.9 (dm, $^1J_{RhP}$ = 203 Hz). ^{19}F NMR (acetone-d_6, 376.05 MHz, 20 °C): δ −78.51 (s, PCF_2CF_3), −110.71 (dd, $^2J_{FF}$ = 301 Hz, $^2J_{FP}$ = 56 Hz), −113.16 (dd, $^2J_{FF}$ = 301 Hz, $^2J_{FP}$ = 56 Hz).

$[(dfepe)Ir(\mu\text{-}Cl)]_2$ (2). In a procedure analogous to that described for **1**, a solution of $[(C_8H_{12})Ir(\mu\text{-}Cl)]_2$ (0.250 g, 0.372 mmol) in toluene was treated with dfepe (0.501 g, 0.885 mmol). After 2 h, 0.537 g (91%) of **2** was obtained as a yellow crystalline precipitate. Anal. Calcd for $C_{20}H_8Cl_2F_{40}Ir_2P_4$: C, 15.13; H, 0.51. Found: C, 15.43; H, 0.40. IR (cm^{-1}): 1339 vw, 1298 s, 1228 s, 1209 s, 1127 s, 969 w. ^1H NMR (acetone-d_6, 269.7 MHz, 20 °C): δ 2.53 (m, PCH_2). ^{31}P NMR (acetone-d_6, 161.9 MHz, 20 °C): δ 67.5 (ps. p, $^2J_{FP} \approx 55$ Hz). ^{19}F NMR (acetone-d_6, 376.05 MHz, 20 °C): δ −78.70 (s, PCF_2CF_3), −112.54 (dd, $^2J_{FF}$ = 320 Hz, $^2J_{FP}$ = 53 Hz), −115.14 (dd, $^2J_{FF}$ = 320 Hz, $^2J_{FP}$ = 58 Hz).

CpIr(dfepe) (3). A 0.200-g (0.0126-mmol) sample of **2** and 0.097 g (0.0360 mmol) of TlCp were combined in 30 mL of THF and refluxed for 12 h, during which time the solution changed from yellow to orange. The solvent was removed under vacuum and the residue was extracted with diethyl ether. Reduction of the filtrate to ca. 2 mL and cooling to −78 °C yielded an orange solid which was isolated by cold filtration and dried under vacuum. The yield was 0.125 g (60%) of **3**. Anal. Calcd for $C_{15}H_9F_{20}IrP_2$: C, 21.88; H, 1.10. Found: C, 22.21; H, 1.04. IR (cm^{-1}): 1290 vs, 1202 vs, 1120 vs, 962 s, 820 m, 747 m, 712 m, 681 w, 644 vw, 626 w, 550 w, 517 s, 484 m. ^1H NMR (benzene-d_6, 400 MHz, 22 °C): δ 4.95 (s, 5H; C_5H_5), 1.66 (m, 4H; PCH_2). ^{31}P NMR (benzene-d_6, 161.9 MHz, 20 °C): δ 67.6 (m). ^{19}F NMR (benzene-d_6, 376.05 MHz, 20 °C): δ −77.24 (s, PCF_2CF_3), −113.92 (dd, $^2J_{FF}$ = 318 Hz, $^2J_{FP}$ = 51 Hz), −117.16 (dd, $^2J_{FF}$ = 318 Hz, $^2J_{FP}$ = 59 Hz).

(dfepe)Ir(NEt_2H)Cl (4). A 0.300-g (0.209-mmol) sample of **2** was dissolved in 15 mL of dry NEt_2H and stirred at ambient temperature. After 30 min the volatiles were removed under vacuum and the residue was sublimed at 80 °C at 10^{-4} Torr. A 0.150-g (83%) yield of analytically pure lemon-yellow crystalline **4** was obtained. Anal. Calcd for $C_{14}H_{15}ClF_{20}IrNP_2$: C, 19.40; H, 1.74. Found: C, 19.72; H, 1.66. IR (cm^{-1}): 3197 w, 1296 s, 1225 vs, 1206 sh, 1125 s, 969 s, 807 w, 749 m, 714 m. ^1H NMR (benzene-d_6, 269.7 MHz, 20 °C): δ 3.71 (br. s, 1H;

(33) Miller, J. S.; Epstein, A. J. *Prog. Inorg. Chem.* **1976**, *20*, 76–78.

(34) (a) Herde, J. L.; Lambert, J. C.; Senoff, C. V. *Inorg. Synth.* **1974**, *15*, 18. (b) Chatt, J.; Venanzi, L. M. *J. Chem. Soc.* **1957**, 4735.

$(CH_3CH_2)_2NH$), 3.03 (dqd, $^2J(H_b)$ = 12.8 Hz, $^3J(NH)$ = 6.8 Hz, $^3J(CH_3)$ = 6.4 Hz, 2H; $(CH_3CH_aH_b)_2NH$), 2.54 (dqd, $^2J(H_a)$ = 12.8 Hz, $^3J(NH) \approx 6$ Hz, $^3J(CH_3) \approx 6$ Hz, 2H; $(CH_3CH_aH_b)_2NH$), 1.44 (m, 4H; PCH_2), 0.80 (dd, $^3J(HH_a)$ = 6.4 Hz, $^3J(HH_b) \approx 6$ Hz, 6H; $(CH_3CH_2)_2NH$). ^{31}P NMR (benzene-d_6, 161.9 MHz, 20 °C): δ 69.5 (m), 61.5 (m). ^{19}F NMR (benzene-d_6, 376.05 MHz, 20 °C): δ −78.17 (s, PCF_2CF_3), −78.86 (s, PCF_2CF_3), −111.16 (dd, $^2J_{FF}$ = 312 Hz, $^2J_{FP}$ = 38 Hz), −111.55 (dd, $^2J_{FF}$ = 320 Hz, $^2J_{FP}$ = 45 Hz), −113.23 (dd, $^2J_{FF}$ = 312 Hz, $^2J_{FP}$ = 45 Hz), −115.13 (dd, $^2J_{FF}$ = 312 Hz, $^2J_{FP}$ = 75 Hz).

Reactions of [(dfepe)M(μ-Cl)]$_2$ with CO. A 0.080-g sample of **2** was dissolved in 10 mL of THF and placed under 1 atm of CO. The light yellow solution became pale green after being exposed to CO for several minutes. After 14 h, the volatiles were removed and the residue was extracted with ether. Concentration of the filtrate to ca. 2 mL and precipitation at −78 °C yielded 0.072 g of a yellow solid which consisted of a 80:20 mixture of (dfepe)Ir(CO)Cl (**5**) and **2**, as judged by ^1H and ^{31}P NMR. NMR analysis of a sample of this mixture after refluxing in benzene under nitrogen for 30 min indicated a quantitative conversion to **2**. The isolation of (dfepe)Rh(CO)Cl (**6**) was not attempted due to its correspondingly higher CO lability. Spectral data for **5**: IR (cm^{-1}): 2086 vs, 1299 vs, 1229 vs, 1207 s, 1132 vs, 969 vs, 808 w, 752 m. ^1H NMR (benzene-d_6, 269.7 MHz, 20 °C): δ 1.55 (m; PCH_2). ^{31}P NMR (benzene-d_6, 161.9 MHz, 20 °C): δ 76.4 (m), 68.0 (m). ^{13}C NMR (acetone-d_6, 100.5 MHz, 20 °C): δ 178.55 (dd, $^2J_{PC}$ = 8, 142 Hz). Spectral data for **6**: IR (acetone): 2093 cm^{-1}. ^1H NMR (acetone-d_6, 400 MHz, 20 °C): δ 3.05 (m; PCH_2). ^{31}P NMR (acetone-d_6, 161.9 MHz, 20 °C): δ 98.1 (m), 87.3 (m).

X-ray Structure Determinations. X-ray data sets were collected at −100 °C on a Siemens R3m/V automated diffractometer system with a dedicated Microvax II computer system and fitted with an LT-2 low temperature device. The radiation used was Mo Kα monochromatized by a highly-ordered graphite crystal. The parameters used during data collections are summarized in Table II. All computations used the SHELXTL PLUS (Version 3.4) program library (Siemens Corp., Madison, WI).

[(dfepe)M(μ-Cl)]$_2$ (M = Rh, 1; M = Ir, 2). Suitable crystals of both **1** and **2** were obtained as well-formed blocks from acetone solution. Hexagonal unit cell dimensions were derived from least-squares fitting of random reflections (18° ≤ 2θ ≤ 28°). Data sets were collected using the ω scan technique. Three standard reflections monitored after every 100 data collected showed no systematic variation. Analyses of systematic absences for the total data sets indicated that the crystal system was trigonal in each case. Although the data did not yield an unambiguous space group assignment, the successful refinement of both structures in $P3_221$ confirmed that the initial choice of this space group was correct; refinements in the enantiomeric space group $P3_121$ resulted in a higher final R value in both cases. Absorption corrections using empirical ellipsoidal models based on φ-scan data collected were applied for both **1** and **2**.

The initial structure solutions for **1** and **2** were solved using direct methods. All nonhydrogen atoms were located on a series of difference Fourier maps. All non-hydrogen atoms of **1** were refined anisotropically; only the iridium, chlorine, and phosphorus atoms of **2** were refined anisotropically due to data/parameter limitations. The dfepe ligand hydrogen atom positions were added in ideal calculated positions with d(C–H) = 0.96 Å and with fixed isotropic thermal parameters set at approximately 1.2 to 1.4 times the isotropic equivalent of the attached carbon atom. Full-matrix least-squares refinement gave final R values of 0.063 (R_w = 0.066; 4009 data, $I > 2\sigma(I)$) for **1** and 0.063 (R_w = 0.065; 2431 data, $I > 2\sigma(I)$) for **2**. The final difference Fourier map for **1** showed a residual electron density peak of 1.67 e/Å^3 associated with the C(5) fluorocarbon unit, with all other maxima or minima less than 1.0 e/Å^3. Several residual density peaks ≤1.79 e/Å^3 were present on the final difference Fourier map for **2** which were associated with the iridium and chlorine atoms and attributable to uncompensated absorption.

(dfepe)Ir(NEt$_2$H)Cl (4). Yellow plates of **4** were grown from dichloromethane solution by slow evaporation. Orthorhombic unit cell dimensions were derived from a least-squares fit of 50 random reflections (20° ≤ 2θ ≤ 30°). Data were collected using the 2θ/θ scan technique and exhibited no systematic variation. Analysis of systematic absences for the total data set indicated that the correct space group was $P2_12_12_1$. The absolute configuration chosen for **4** in this space group was verified as correct using an anomalous dispersion multiplier test.[35] Data were corrected for absorption empirically, as described previously.

The structure solution and refinement procedures were the same as above. All nonhydrogen atoms were refined anisotropically, with dfepe backbone and amine ethyl hydrogen atom positions placed in idealized positions with fixed isotropic thermal parameters. The amine hydrogen was not located on difference maps and was not included in the model. Full-matrix least-squares refinement gave an R value of 0.038 (R_w = 0.041) for all 3971 observed data. The final difference Fourier map showed absorption fringes of 2.30 and 1.30 e/Å^3 symmetrically disposed about the iridium center.

Acknowledgment. This work has been supported by the National Science Foundation (Grant No. CHE-8912697) and the donors of the Petroleum Research Fund, administered by the American Chemical Society. Johnson Matthey is gratefully acknowledged for a generous loan of iridium and rhodium trichlorides.

Supplementary Material Available: Tables of complete X-ray data collection parameters, atomic coordinates, bond distances, bond angles, anisotropic thermal parameters, and hydrogen atom coordinates and isotropic thermal parameters for **1**, **2**, and **4** (Tables S1–S18) (31 pages). Ordering information is given on any current masthead page.

(35) Rogers, D. *Acta. Crystallogr., Sect. A* **1981**, *37*, 734.